https://doi.org/10.5194/nhess-2020-240
Preprint. Discussion started: 1 September 2020

Natural Hazards and Earth System Sciences
Discussions

Assessing heat exposure to extreme temperatures in urban areas using the Local Climate Zones classification

Joan Gilabert[1,2,3], Anna Deluca[4], Dirk Lauwaet[5], Joan Ballester[4], Jordi Corbera[2], Maria Carmen Llasat[1]

[1]GAMA Team Department of Applied Physics - University of Barcelona,
[2] Institute Cartographic and Geological of Catalonia (ICGC),
[3]URBAG research team, Sostenipra SGR 1412 ICTA-UAB,
[4]Climate and Health Program - Barcelona Institute for Global Health,
[5]Flemish Institute for Technological Research (VITO)

Correspondence to: Joan Gilabert (jgilabert@meteo.ub.edu)

Abstract. Trends of extreme temperature episodes in cities are increasing (in frequency, magnitude and duration) due to regional climate change in interaction with the urban effects. Urban morphologies and thermal properties of the materials used to build them are factors that influence the spatial and temporal climate variability and becomes one of the main reasons for the climatic singularity of cities. This paper presents a proposal to evaluate the urban and peri-urban effect on extreme temperatures exposure in Barcelona (Spain), using the Local Climate Zone (LCZ) framework as a base statement, that allows the comparison with other cities of the world characterized using this criterion. LCZs were introduced as input of the high resolution UrbClim model (100 m spatial resolution) to create the daily temperatures (median and maximum) series for summer (JJA) during the period 1987 to 2016, pixel by pixel, in order to create a cartography of extremes. Using the relationship between mortality due to high temperatures and the temperature distribution, the heat exposure of each LCZ was obtained. Methodological results of the paper show the improvement obtained when LCZs were mapped through a combination of two techniques (from Land Cover/Land Use maps and from WUDAPT method), as well as proposes a methodology to obtain the exposure to high temperatures of different LCZs on urban and peri-urban areas. In the case of Barcelona, the distribution of temperatures for the 90th percentile (about 3-4ºC compared to average conditions) leads to an increase in the relative risk of mortality of 80%.

https://doi.org/10.5194/nhess-2020-240
Preprint. Discussion started: 1 September 2020

1. Introduction

Alterations to the natural environment associated with urban activity mean that climate variability in urban landscapes is more complex than in peri-urban and rural areas. Urban landscapes are home to more than half the world's population and projections show that two-thirds of the world's population will live in cities by 2050 (UN, 2015). Urban areas are certainly more exposed and vulnerable to the negative effects of climate change due to their non-sustainable relationship with surrounding areas and environments. The Urban Climate Change Research Network's Second Assessment Report on Climate Change in Cities (ARC 3.2) (Rosenzweig et al., 2018), places the average annual temperature increase ratio per decade between 0.12 and 0.45ºC in the period from 1961 to 2010. And it is estimated that the temperature will rise between 1.3 and 3ºC towards 2050 and 1.7 to 4.9ºC in 2080.

Urban landscapes are particularly sensitive to rising temperatures at all timescales (Pachauri RK et al., 2014). Heat waves (HW) are one of the deadliest weather events and their frequency, intensity and duration are expected to increase in the future due to climate change (Li and Bou-Zeid, 2013; De Jarnett and Pittman, 2017; Sheridan and Dixon, 2016) and the urban heat island (UHI) effect. Consequently, the related health impacts are of emerging environmental health concern (Wolf and McGregor, 2013). In Europe, the growing urbanisation along with the impacts of the increasing of extreme temperature causes increased heat-related mortality (Smid et al., 2019; Ingole et al., 2020).

There are many factors that influence the spatial and temporal climate variability in urban areas, such as different urban morphologies and the thermal properties of the materials used to build them (Geletič et al., 2016; Li et al., 2016). One of the main topics usually studied to characterise the urban climate are the extreme temperatures in cities due to UHI effect, which was first discussed back in the 1940s (Balchin and Pye, 1947). Historically, a considerable body of research has been published on the phenomenon (i.e, Oke, 1982; Lo et al., 1997; Arnfield, 2003; Voogt and Oke, 2003; Chen et al., 2006; Mirzaei and Haghighat, 2010; Giannaros et al., 2014; Lehoczky et al., 2017; Sobrino and Irakulis, 2020). However, certain methodological inconsistencies have been revealed when comparing different urban climate studies. One of the main reasons is the lack of standardisation to compare the properties that affect specific urban thermal behaviour

(Stewart, 2011). Moving forward from this premise, a new methodology based on the Local Climate Zone (LCZ) classification has emerged (Stewart and Oke, 2012). LCZ establishes a system of standardisation for urban and rural areas and their thermal responses. LCZ proposes a classification with a total of 17 measurable categories based on a combination of geometric, thermal, radiative and metabolic parameters that characterise urban and peri-urban areas (Fig. S1). By using this classification, it is possible to study the effects of urban climate in more spatial and temporal detail (Bechtel et al., 2015). The combination of built environment (Benzie et al., 2011; Inostroza et al., 2016) is well encompassed by the LCZ approach, and, along with socio-demographic factors (Nayak et al., 2018), this allows us to develop a geospatial distribution of heat exposure (Dickson et al., 2012; Drobinski et al., 2014). Along the same line of research, the international project called World Urban Database and Access Portal Tools (WUDAPT) has created a portal with guidelines based on earth observation data, with the aim of building a worldwide database of cities, using the LCZ classification. This standardisation will allow comparisons between cities, while providing better data for meteorological and climate models (Brousse et al., 2016; Ching et al., 2018). Currently, the available, validated layer for Barcelona on the WUDAPT portal is the one made in our studio to fill in the Metropolitan Area of Barcelona (AMB), as explained in more detail in section 3.1.

Although the LCZ was originally designed to describe the radiative characteristics of the different land covers and land uses, it can also be applied to estimate the level of heat exposure to adverse climate conditions. There are a wide range of definitions for the term 'vulnerability' (UNISDR, 2009; Cutter, 1996; Llasat et al., 2009), which depend on different physical and social factors (Cutter et al., 2000; Tromeur et al., 2012; Nakamura and Llasat, 2016). In this framework heat vulnerability is understood as a combination of heat exposure (based on high temperatures) and sensitivity (Wolf and McGregor, 2013; Bao et al., 2015; Inostroza et al. 2016), where the last is related with the population characteristics and coping capacities. Although there are some publications that study risk on an urban scale for extreme heat events (Xu et al., 2012; Weber et al., 2015; Krstic et al., 2017; Eum et al., 2018), few have been studied from an LCZ perspective. This paper therefore aims to assess heat exposure using the LCZ classification in a coastal Mediterranean metropolitan region. Barcelona constitutes a good example of a Mediterranean coastal megacity (port cities with a population greater than 1 million in

https://doi.org/10.5194/nhess-2020-240
Preprint. Discussion started: 1 September 2020

Natural Hazards and Earth System Sciences
Discussions

2005) (Hanson et al., 2011) that can be severely affected by climate change impacts. In effect, annual mean temperature increase in the Mediterranean Basin is higher than the world average (1.5ºC above 1880-1899 in 2018) and could be above 2.2ºC in 2040 without additional mitigation (Lionello et al., 2014; Cramer et al., 2018; MedECC, 2019). Direct impacts on health produced by the frequency and intensity increase of heat waves and tropical nights will be amplified by the urban heat island effect, particularly important in Barcelona (Baccini et al, 2011; Martin-Vide and Moreno, 2020). Associated to this temperature increase, by 2050, for the lower sea-level rise scenarios and current adaptation measures, cities in the Mediterranean will account for half of the 20 global cities with the highest increase in average annual damages (Hallegate et al., 2013).

The paper is divided into two main chapters. The first deals with the study area, data and proposed methodology. The second, is focused on applying the methodology to the city of Barcelona and showing the respective results. The paper ends with a section on discussion and conclusions.

This study is a starting point for new research lines with three objectives in mind: a) making changes to urban land cover and observing the changes in heat exposure to high temperatures without having to resort to climate modelling; b) downscaling the temperature outputs of urban models to resolutions under 100m using the LCZ maps; c) applying this methodology to climate change scenarios.

2. Data and Methods

2.1. Study area

The Metropolitan Area of Barcelona (AMB) and its surroundings have been selected to apply the LCZ classification. AMB involves the city of Barcelona and 35 adjoining municipal areas (Fig. 1). The AMB is situated in the northwest of the Mediterranean basin and covers an area of 636 km^2 with a population of around 3,2 million. The city of Barcelona (~1,6 million) is in its centre, between the Llobregat River (South), the Besòs River (North), the Catalan Coastal Range (West) and the Mediterranean Sea (East) (Fig. 1b).

The Barcelona municipality has been selected to analyse the effect of high temperatures and apply the proposed methodology approach on a neighbourhood scale. Barcelona is divided into 10 districts, which are subdivided into 73 neighbourhoods. It covers an area of 101 km^2 and has a population density of over 15,000 inh./km^2, which is higher than New York City, Tokyo or New Delhi. In terms of climate, Barcelona and its surroundings are characterised by hot summers (25ºC-27ºC average temperature), and the thermal stress of high temperatures is accentuated by the proximity of the sea, which results in a humid atmosphere. Total precipitation in Barcelona is around 600 mm per year. Autumn is the wettest season and has a highly irregular distribution of precipitation, in many cases causing episodes of urban flooding (Gilabert and Llasat, 2017; Cortès et al., 2018).

2.2 Methodology design

In order to carry out this study, we followed the workflow shown below:

1. LCZ Mapping: A GIS methodology based on Land Cover and Land Use (LCLU) maps has been applied to the entire AMB to improve the precision of the international WUDAPT method. The WUDAPT method has been also applied to all the area showed in Figure 1b, both inside and outside AMB, that will be used as input of the climate model.
2. Climate characterisation of the median and extreme temperature distribution in Barcelona from the outputs of UrbClim model.
3. Defining the heat exposure thresholds based on the epidemiological temperature-mortality model proposed by Achebak et al. (2018).
4. Developing a methodology for the thermal characterisation of the LCZs and its assessment.

Each one of these steps will be explained in detail in the following sections in order to simplify the understanding of this methodology in which each part is based in the results of the previous one. The own methodology followed constitutes a result of this work.

2.3. LCZ mapping

2.3.1 Data from official thematic cartography, satellite images and weather stations

https://doi.org/10.5194/nhess-2020-240
Preprint. Discussion started: 1 September 2020

Natural Hazards and Earth System Sciences
Discussions

In order to create the LCZ cartography data showed in Table 1 have been used. The LCZs were represented following two methods, as explained in section 3. The Land Cover Land Use method was based on using all the layers presented in Table 1, except for the Landsat 8 image, which was only used with the WUDAPT methodology and the orthophoto to make the training areas.

2.3.2 Land Cover and Land Use method and WUDAPT method

There are several proposals for mapping LCZs, whether from a bottom up or top down approach (Brousse et al., 2016; Lelovics et al., 2014; Wang et al., 2017; Mitraka et al., 2015). Each LCZ is defined by 10 variables (geometric, radiative and metabolic), which were tested and standardised by Stewart and Oke (2012) and are applied in this study.

Our study features a LCZ map that combines two different mapping techniques (Fig. 2). For the administrative region of the AMB (with a more extensive and detailed source of data), a methodology based on LCLU data was used that departs from the reclassification of the land use key for the existing high-resolution maps. The LCLU data were combined with LIDAR data, which allowed us to define the height of the buildings. There are other techniques that use similar methodologies to show LCZs, like those by Geletič and Lehnert (2016) or Skarbit et al. (2017). For the area outside the AMB, the international WUDAPT methodology was used, based on satellite earth observation data (Bechtel et al, 2015). This study improved accuracy through a population map and high resolution orthophotos provided by the Cartographic and Geological Institute of Catalonia (ICGC). Both methodologies are summarized below.

The LCLU method is based on different Land Cover and Land Use maps (see Table 1), such as the Land Cover Map of Catalonia (LCLU-Cat), which uses an extensive classification of up to 241 categories (CREAF, 2010), and the Urban Atlas (UA) (EEA, 2010). The first thematic map was used to define the Land Cover Types and density of vegetation. The UA distinguishes 20 categories of urban areas and discerns between urban fabric type and density, which is why it is very useful for the first 10 categories of LCZ. Each LCLU category corresponds to one of the descriptions of the different morphological parameters that define the LCZ. The Building Heights is another layer of the map, and was made with a LIDAR sensor, which was also used to discern between the different Urban Climate Zones.

https://doi.org/10.5194/nhess-2020-240
Preprint. Discussion started: 1 September 2020

Natural Hazards and Earth System Sciences
Discussions

Figure 3 shows the difference between the total coverage of each LCZ when obtained from the LCLU and from WUDAPT maps in AMB (Fig. 2). In the WUDAPT approach, 52.8% of the surface area of the AMB consists of urban areas (LCZ 1-10 and E), while in the high-resolution map (LCLU approach), the same type of coverage occupies just 37.3% due to the different resolution of both methodologies. In both methods, we can see that the natural forest category (LCZ-A) is the most common, accounting for 24.1% and 18.4% of the land respectively. This is due to the fact that the AMB includes Collserola Natural Park in the Coastal Mountain Range. The next most common class is LCZ-C, which corresponds to scrubland and bush. Dealing with land classified as urban, the most common types include industrial estates (LCZ-8), areas with dense buildings less than 25 m tall (LCZ-2) and category LCZ-6, which consists of open arrangements of mid-rise buildings. The WUDAPT map suffers from a lack of characterisation of urban areas, which is not the case for the LCLU map.

The resulting LCZ map is a high resolution thematic/vector map/base map (Figure 2b), in which each polygon that makes up the urban fabric is attributed to an LCZ category (Gilabert et al., 2016). Finally, it was rasterised at a resolution of 100 m, applying an all shape filter, so that it could be used as an input for the UrbClim model. The method we followed is shown in the workflow diagram (Figure 4). There are similar examples in the literature, such as the LCZ map for the Ïle-de-France (www.institutparisregion.fr), or the LCZ-LCLU Map of Vienna (Hammerberg et al., 2018).

The WUDAPT method (Bechetel et al., 2015) allows us to create a 100 m x 100 m raster map based on earth observation data from remote sensing. The representative regions of interest are chosen for proposed LCZ categories from earth observation satellite data, with the use of very high resolution aerial orthophotos as a ground truth. The LCZ map, made by the first author of this paper, using the WUDAPT proposal, is officially presented on the project portal and is available for download (www.wudapt.org). This method has been applied to an extended area as is showed at Figure 5.

A multi-resolution grid shape file (62.5 m, 125 m and 250 m) containing information on the population as registered in 2016 (IDESCAT, 2018) was used to correct the peri-urban areas of AMB where rural activities cannot see well identified. The orthophoto was used to check and correct any categories and the limits between them.

Figure 5 shows the resulting map combining the LCLU method (in raster format) for the administrative region of the AMB, and WUDAPT method for the rest of the study area with a final resolution of 100m.

2.4 Weather stations

Table 2 shows the weather stations within the municipality of Barcelona that have been used to evaluate and compare the characterization of the LCZ with the daily average temperature outputs of the UrbClim model. LCZ and height information are also attached.

2.5 UrbClim model simulation

UrbClim is an Urban Boundary-Layer Climate Model specifically designed to simulate temperature at a very high spatial resolution (here at 100 m; De Ridder et al., 2015). The model consists of a land surface scheme with simplified urban physics coupled to a 3D atmospheric boundary layer. UrbClim is faster than high-resolution mesoscale climate models by at least two orders of magnitude (García-Díez et al., 2016), making the very long runs that are necessary for climate change related studies possible. UrbClim has been recently validated in several European cities, including Barcelona (García-Díez et al., 2016). Currently, within the framework of the Pan-European Urban Climate Service (PUCS) project (H2020, 2017-2010), the urban climate of Barcelona has been modelled until 2100, keeping in mind different Representative Concentration Pathways (RCPs) to observe the consequences of climate change on an urban scale. Barcelona was chosen, among other European cities, and VITO and ISGlobal were the organisations responsible for modelling this city.

UrbClim model uses a land-surface and a soil-vegetation-atmosphere transfer scheme that is designed to deal with urban surfaces. Each surface grid cell in the model is made up of portions of vegetation, bare soil and urban surface cover, which are all represented using LCZ mapping. A set of transfer equations, together with appropriate parameter values for albedo, emissivity, aerodynamic and thermal roughness length are used to simulate the heat transfer in each surface grid cell. The large-scale atmospheric conditions are used as lateral and upper boundary conditions. The 3D boundary layer model represents a simplified atmosphere by using the continuity equations for horizontal momentum, potential temperature, specific humidity and mass.

The simulations for the 1987-2016 period were used for this period. The UrbClim simulations cover a large domain containing 401x401 horizontal grid points at 100 m resolution (40x40 km approximately), and 19 vertical levels within the lower 3 km of the troposphere. It covers the entire geographical area of the Metropolitan Area of Barcelona, including the neighbouring highly populated cities. The driving model data are updated every 3 hours using ERA-Interim reanalysis (Dee et al., 2011), which runs at a spatial resolution of T255 (approximately 70-80 km). The UrbClim model directly downscales the ERA-Interim reanalysis data to 100 m resolution. The climate distribution of the daily mean temperature (Tmean), maximum temperature and dew point temperatures were calculated for all the summer months (JJA). The dew point temperature (Tdew) was used as a starting point to calculate the HUMIDEX Eq. (1) that describes the perceived thermal feeling of a person, by combining the effect of heat and humidity (Masterton and Richardson, 1979). Barcelona has quite a high relative humidity during the summer months, which means that the HUMIDEX increases considerably.

$$HUMIDEX = T_{mean} + 0.5555\ [6.11 e^{5417.7530\left(\frac{1}{273.16}+\frac{1}{273.15+T_{dew}}\right)} - 10] \quad \text{Eq. (1)}$$

2.6 Quantifying heat exposure by temperature

The next step consists of reclassifying the maps of the proposed distributions for the daily mean temperature, keeping in mind the impact that they can have on the health. This was carried out using the results provided in the study by Achebak et al. (2018), in which a distributed lag nonlinear model was used to model the short-term delayed relation between daily summer temperature and mortality data from cardio-respiratory diseases in Barcelona (and 46 other cities), over a similar period of time modelled (Fig. 6). This makes it possible to objectively establish the thresholds for health relative risks (RR), based on temperature. For instance, a RR value of 1.20 means that the relative risk of mortality is 20% higher at a given level of temperature exposure compared to a baseline optimum temperature (e.g. temperature of minimum mortality, when RR=1). Relative risks are statistically significant when the lower bound of the CI is greater than 1.

We are assuming that the curve is applicable to all districts of the city (Achebak et al., 2018). Table 3 has been built for RR intervals of 0.2 (20%) following the Figure 6. Each RR interval has been associated to a Heat Exposure Index (HEI) that includes temperature

https://doi.org/10.5194/nhess-2020-240
Preprint. Discussion started: 1 September 2020

Natural Hazards and Earth System Sciences Open Access
Discussions

interval based on the curve of Achebak et al. (2018). Barcelona deals with HEI value of 1 for temperatures between 18 and 20ºC up to a HEI value of 7, for temperatures above 31.1ºC that would mean a very high relative risk of mortality associated with high temperatures.

3. Results

3.1 UrbClim temperature outputs and HEI maps

In order to analyse the impact of the different LCZ in the distribution of high temperatures in summer the maps of maximum and daily mean temperature corresponding to percentiles P50, P75, P90, P95 and P99 have been built (Fig. 7). Barcelona has a high relative humidity due to proximity to the sea that increases the warm perception, and, for this reason, the cartography of the average daily HUMIDEX value has also been represented.

As we can see in figure 7, there is a very similar spatial distribution pattern. The lowest temperatures are in the most remote area of the coast and they are mainly associated with categories LCZ A and LCZ 9 (mainly covering areas of woodland or very low-density buildings). A cooling effect can also be noted in the most important parks in the city, as well as on the seafront, because of the sea breeze (the UrbClim model underestimates the sea breeze effect in Barcelona, García-Diez et al., 2016). The highest temperatures can be found in the centre of the city, with a tendency to increase in a north-easterly direction.

We saw that P99 of HUMIDEX reached 39ºC. In Barcelona, without taking humidity into account, the average temperature in the city can reach above 30ºC. Even so, normal temperatures during the summer are around 27ºC. In Mediterranean cities, relative humidity is important since it is usually high, a fact that affects temperature (Diffenbaugh et al., 2007). In this sense, we observe that the HUMIDEX can register temperatures of the order of 5ºC higher than the sensible temperature. Anyway, this study has focused on sensible temperature because the curve that defines the HEI has been made for sensible temperature. In any case, we must bear in mind that the temperature or heat stress may be higher due to the greater HUMIDEX.

Figure 8 shows maps of HEI distribution reclassified the UrbClim output of daily mean temperature according to the proposed thresholds showed in section 2.6. This

https://doi.org/10.5194/nhess-2020-240
Preprint. Discussion started: 1 September 2020

reclassification turns the extreme temperature maps or hazard maps into heat exposure maps. It can be seen that the HEI is lower in areas with higher altitude and in inter-urban parks (as the Montjuïc Park located in SE of the map), although when P90 is surpassed, the HEI value goes over level 5 for most of the urban fabric. Note that the P50 shows an increase in the relative risk of mortality of 40%.

3.2 Thermal characterisation of the LCZs

In this section we aim to match up each LCZ with a determined thermal behaviour to create a methodology that will allow us to estimate the heat exposure to high temperatures from this data.

First, we analysed the thermal response of the LCZ (LCZ-T) to the high temperature situations obtained in the climate analysis (Fig. 7). Second, we analysed the probability density curves for each LCZ, so that we could calculate the anisotropy levels of the LCZs. Using this foundation, we built curves for the LCZs and a defined scenario for the percentiles considering the HEI, which allowed us to create a model that was applicable not only to Barcelona but also to other regions with similar behaviour. Transposing the model on LCZ maps allows us to map heat exposure distributions for Barcelona.

Figure 9 shows that LCZ 8, 1, E and 2 (from highest to lowest), have usually the highest temperatures. These LCZ in general terms correspond to the categories with high admittance and high permeability (Stewart and Oke, 2012). In contrast, the lowest temperatures correspond to LCZ 9, A, C and G, which are wooded areas and parks on the outskirts of the city. On the other hand, crops and bare land (LCZ C and F) show very variable behaviour, as during the day they tend to be surfaces that store and retain heat, while during the night their behaviour registers temperatures under the average of the sample. These surfaces are characterised by a large temperature range given the marked contrast between day and night.

Table 4 shows that the more extreme the percentile the larger the standard deviation, as expected. Besides this, the more marked deviations correspond to LCZ C and F, which correspond to wooded or bare areas and which show less thermal inertia. On the other hand, category C is very highly influenced (in the case of Barcelona) by orientation, as there are zones located in shaded parts of valleys while other zones are in the sunny ones,

https://doi.org/10.5194/nhess-2020-240
Preprint. Discussion started: 1 September 2020

which has a direct impact on the deviation. In the case of category C, we observed that it corresponds to a land use that is not very representative in spatial terms.

3.3 Mapping the heat exposure with LCZs

Figure 10 shows the average behaviour of the LCZs for different temperature percentiles (P50, P75, P90, P95, P99). The values corresponding to range between the 25th and 75th percentiles of each LCZ for each probability scenario have been adjusted to a logarithmic curve that can be very useful to build heat exposure maps for high temperatures based on the thermal properties of the LCZ. Knowing the temperature distribution for each category and scenario allows doing the simulation of the impact on temperature distribution of potential modifications to the urban morphology.

As explained in the methodology, seven ranges of temperature have been defined according to different relative risk thresholds (Table 3) established by the curve proposed in the study by Achebak et al. (2018) (Fig. 6). By characterising the LCZ from the model represented in Figure 11, the maps of the heat exposure index (HEI) associated to high temperatures for different probabilistic scenarios have been built. The scenario corresponding to the P75 of the temperature would imply a ratio of relative risk of mortality increase of 60%, and, 80% in a scenario according to the P90.

3.4 Assessment and comparation of the LCZ-T relationship

The results of the LCZ-T relationship as well as the results of the Urban Climate model (UC) have been compared with the distribution of temperature obtained from series of over 10 years for five weather stations (Table 2) located in different LCZ in the municipality of Barcelona. RMSE and the differences between the output of both (UrbClim model and LCZ-T relationship) and observations have been obtained in order to compare the results (Tables 5 and 6). We want to highlight that the UrbClim has been already validated in Barcelona by García-Díez et al. (2016) as outlined in section 2.6. Table 5 shows that differences in absolute value are lower than 1.2ºC. In all the cases they are equal or below 0.5 ºC for the percentile of 50, and also for the percentile of 75 with the exception of the Raval station, that is placed in the oldest part of the city. It should also be kept in mind that a standalone observation is not the same as an aerial 100 x 100

https://doi.org/10.5194/nhess-2020-240
Preprint. Discussion started: 1 September 2020

m observation, and this fact is particularly important when the weather station is surrounded by buildings.

The HEI maps drawn up using the LCZs were compared with the map based on temperature distributed created by UrbClim (Table 6). Coincidences between pixels for both models are above 80% for percentiles P50, P75 and P90, and more than 60% in all cases.

4. Discussion and conclusions

Along this paper a methodology to characterize the distribution of daily mean temperature for the different LCZs in different scenarios has been proposed. This characterization has been done for the summer months and climate percentiles have been obtained for the period 1987-2016 and applied at 100 m resolution to the city of Barcelona. Although other authors have already worked with the relationship between thermal behaviour and LCZ category (Stewart et al., 2014; Skarbit and Gal., 2015; Geletič et al., 2016; Verdonck et al., 2018) they have usually applied Land Surface Temperature satellite images, for the summer months and a short time period. Other characterizations of LCZ using weather stations can also be found in Alexander and Mills (2014) and Kotharjar and Bagade (2018). In this case, these authors have worked with climate series from observational data. The advantage of the methodology proposed here, in which the LCZ distribution has been compared with the outputs of a high-resolution climate model (UrbClim) is that the relationship has been established from long climate series and for the entire selected region. Currently, there are quite a few studies characterizing LCZs using urban model outputs (Aminipouri et al., 2019; Beck et al., 2018; Geletič et al., 2018; Kwok et al., 2019; Unger et al., 2018), but there are few that do it with climatic outings that span so many years.

The results of this methodology applied to the Metropolitan Area of Barcelona have showed a major difference between the thermal response in summer for the different LCZ that this obtained from some satellite images. In terms of land use, LCZ A and C, that belong to the most prevalent categories, show the lowest temperatures, consistent with the majority of studies carried out (e.g. Geletič et al., 2016). In our case, category C

https://doi.org/10.5194/nhess-2020-240
Preprint. Discussion started: 1 September 2020

Natural Hazards and Earth System Sciences
Discussions

shows a wider interquartile range than the other types. This is because this category is found in different altitudes along the Catalan Coastal Range and in areas with different orientations. Regarding category B, attributed to the majority of interurban parks, it maintains temperatures below those of the most typical urban zones.

The highest daily mean summer temperatures in Barcelona are concentrated in LCZ 2, E, 1, 8 F and 10, with LCZs 2, 1 and E being the most representative of the urban planning in the city centre. With regard to LCZ 8 and 10, these are zones that tend to record high temperatures due to the nature of the activities and materials on the land cover (in the most cases, metal structures). The urban LCZ with the lowest temperatures is 9, which is almost non-existent in Barcelona and is located mainly in zones in the Catalan Coastal Range with a significant altitudinal slope. Another urban LCZ with low relative temperatures commonly found in the city is 6, which is mainly located in the neighbourhoods furthest away from the coast and closer to the mountain. These neighbourhoods have a higher percentage of urban green cover, less dense buildings and one of the highest per capita GDPs in the city.

The paper has also introduced the Heat Exposure Index (HEI), that evaluates the increase of the risk of mortality ratio as a consequence of heat exposure in basis to the model proposed by Achebak et al. (2018) which connects relative risk of mortality caused by cardio-respiratory failure with the effects of high temperatures. This index, associated to each LCZ once the temperature has been associated to it, allows mapping the HEI. The comparison between the HEI maps elaborated directly from the temperature outputs produced by the UrbClim model and those produced from LCZ cartography is well-suited to simulate them for scenarios corresponding to percentiles of temperature between 50% and 90%, and, in the case in which there is no coincidence between the HEI value in the pixel, it is more usual underestimation than overestimation. In the case of Barcelona, the distribution of temperatures for the P90 (about 3-4ºC compared to average conditions) leads to an increase in the relative risk of mortality of 80%, and 40% in the case of P50.

This paper also provides comparison of two methodologies to cartography the Local Climate Zones (LCZ). The study area has been mapped using two techniques, the LCLU based on land use maps and the WUDAPT. The LCLU has been applied to the Metropolitan Area of Barcelona and the WUDAPT to the entire region (inside and outside) the AMB. The WUDAPT map suffers from a lack of characterisation of different types of urban areas, which is not the case for the LCLU. Then, when the required data is available it is better to apply the LCLU methodology than the WUDAPT one. In this study, the curve of Achebak et al. (2018) was taken into account, as representative of the whole of Barcelona city. In the future, it would be good to have a similar curve for different districts of the city. However, in future work it would be interesting to represent a sensitivity map taking into account coping capacities based on GDP, social structure of the neighbourhood, etcetera. This would include vulnerability.

In conclusion, the LCZ-T relation based on the characterisation of the average temperature for each LCZ corresponding to different percentile distribution, allows us to consider adaptive methods, proposing changes to more sustainable urban planning, for example the use of green or white cover. The advantage of the proposed methodology is that it allows to obtain a heat exposure distribution for summer temperatures without having to resort climate models, by applying the model of temperature distribution associated to each LCZ. It can be also useful to do different experiments modifying land uses and land coverages over the cartography, and, consequently, the LCZ distribution and their associated HEI. Another possibility is being able to separate the heat exposure levels on an LCZ map with higher spatial resolutions to those used in weather models and climate models.

Acknowledgements

This publication was supported by the Industrial Doctorate Programme (ref. 2015-DI-038) between the University of Barcelona and the Cartographic and Geological Institute of Catalonia, the Water Research Institute (IdRA) at the University of Barcelona, M-CostAdapt (CTM2017-83655-C2-2-R) research projects (MINECO/AEI/FEDER, UE) and ERC Consolidator Grant awarded to Gara Villalba (818002-URBAG). The authors would like to thank the European Environment Agency (EEA), Centre for Ecological Research and Forestry Applications (CREAF) and Metropolitan Area of Barcelona for the land use maps available. We would also like to thank the State Meteorological Agency (AEMET) and the Meteorological Service of Catalonia (SMC) for the weather station data. Finally, we want to thank Hicham for giving us the RR model.

JB gratefully acknowledges funding from the European Union's Horizon 2020 research and innovation programme under grant agreements No 865564 (European Research

https://doi.org/10.5194/nhess-2020-240
Preprint. Discussion started: 1 September 2020

Natural Hazards and Earth System Sciences
Discussions

Council Consolidator Grant EARLY-ADAPT), 727852 (project Blue-Action) and 730004 (project PUCS), and from the Ministry of Science and Innovation (MCIU) under grant agreements No RYC2018-025446-I (programme Ramón y Cajal) and EUR2019-103822 (project EURO-ADAPT).

Author contributions

JG conceived the study, designed and carried out the data analysis and wrote the paper. MCL, JC and JB have participated in defining the analysis and methodology, contributed to interpreting the results, and to writing the paper. DL and AdL have run the UrbClim model and prepare the output data.

Competing interests

The authors declare that they have no conflict of interest.

References

Achebak, H., Devolder, D., and Ballester, J.: Heat-related mortality trends under recent climate warming in Spain: A 36-year observational study. PLoS med. 15(7): e1002617, 2018.

Alexander, P., and Mills, G.: Local climate classification and Dublin's urban heat island. Atmosphere. 5(4): 755-774, 2014.

Aminipouri, M., Knudby, A. J., Krayenhoff, E. S., Zickfeld, K. and Middel, A.: Modelling the impact of increased street tree cover on mean radiant temperature across Vancouver's local climate zones. Urban Forestry & Urban Greening, 39, 9–17, 2019.

Arnfield, A. J.: Two decades of urban climate research: a review of turbulence, exchanges of energy and water, and the urban heat island. Int. J. Climatol. 23(1): 1-26, 2003.

Baccini, M., Kosatsky, T., Analitis, A., Anderson, H.R., D'Ovidio, M., Menne, B., Michelozzi, P., Biggeri, A.: Impact of heat on mortality in 15 European cities: attributable deaths under different weather scenarios. J Epidemiol Commun H, 65, 64-70, 2011.

https://doi.org/10.5194/nhess-2020-240
Preprint. Discussion started: 1 September 2020

Natural Hazards and Earth System Sciences
Discussions

Balchin, W. G. V., and Pye, N.: A micro-climatological investigation of bath and the surrounding district. Q. J. Royal Meteorol. Soc. 73(317-318): 297-323, 1947.

Bao, J., Li, X. and Yu, C.: The construction and validation of the heat vulnerability index, a review. Int. J. Environ. Res. Public Health. 12(7): 7220-7234, 2015.

Beck, C., Straub, A., Breitner, S., Cyrys, J., Philipp, A., Rathmann, J., Schneider, A., Wolf, K. and Jacobeit, J.: Air temperature characteristics of local climate zones in the Augsburg urban area (Bavaria, southern Germany) under varying synoptic conditions. Urban Climate, 25, 152–166, 2018.

Bechtel, B., Alexander, P. J., Böhner, J., Ching, J., Conrad, O., Feddema, J., Mills, G., See, L., and Stewart I.: Mapping local climate zones for a worldwide database of the form and function of cities. ISPRS Int. J. Geo-Inf. 4(1): 199-219, 2015.

Benzie, M., Harvey, A., Burningham, K., Hodgson, N., and Siddiqi, A.: Vulnerability to heatwaves and drought: Case studies of adaptation to climate change in South-west England. Joseph Rountree Foundations, 2011.

Brousse, O., Martilli, A., Foley, M., Mills, G., and Bechtel B.: WUDAPT, an efficient land use producing data tool for mesoscale models? Integration of urban LCZ in WRF over Madrid. Urban Clim. 17: 116-134, 2016.

Chen X. L., Zhao H. M., Li P. X., and Yin Z. Y.: Remote sensing image-based analysis of the relationship between urban heat island and land use/cover changes. Remote Sens. Environ. 104(2): 133-146, 2006.

Ching, J., Mills, G., Bechtel, B., See, L., Feddema, J., Wang, X., Ren, C., Brousse, O., Martilli, A., Neophytou, M., Mouzoudires, P., Stewart, I., Hanna, A., Ng, E., Foley, M., Alexander, P., Aliaga, D., Niyogi, D., Shreevastava, A., Bhalachandran, S., Masson, V., Hidalgo, J., Fung, J., de Fatima Andrad, M., Baklanov, A., Wei Dai, D., Milcinski, G., Demuzere, M., Brunsell, N., Pesaresi, M., Miao, S., Mu, Q., Chen, F., and Theeuwes, N.: World urban data base and access portal tools (WUDAPT), an urban weather, climate and environmental modelling infrastructure for the Anthropocene. Bull. Am. Meteorol. Soc. 99(9): 1907-1924, 2018.

https://doi.org/10.5194/nhess-2020-240
Preprint. Discussion started: 1 September 2020

Natural Hazards and Earth System Sciences
Open Access
Discussions

Cortès, M., Llasat, M. C., Gilabert, J., Llasat-Botija, M., Turco, M., Marcos, R., Martin Vide, J. P., and Falcón L.: Towards a better understanding of the evolution of the flood risk in Mediterranean urban areas: the case of Barcelona. Nat. Hazards. 93(1): 39-60, 2018.

Cutter, S. L.: Vulnerability to environmental hazards. Prog. Hum. Geogr. 20(4): 529-539, 1996.

Cutter, S.L., Mitchell, J. T., and Scott, M. S.: Revealing the vulnerability of people and places: a case study of Georgetown County, South Carolina. Ann. Am. Assoc. Geogr. 90(4): 713-737, 2000.

Cramer, W., Guiot, J., Fader, M., Garrabou, J., Gattuso, J. P., Iglesias, A., Lange, M. A., Lionello, P., Llasat, M. C., Paz, S., Peñuelas, J., Snoussi, M., Toreti, A., Tsimplis, M. N., and Xoplaki, E.: Climate change and interconnected risks to sustainable development in the Mediterranean. Nat. Clim. Change 8:972-980, doi: 10.1038/s41558-018-0299-2, 2018.

Dee, D. P., Uppala, S. M., Simmons, A. J., Berrisford, P., Poli, P., Kobayashi, S., Andrae, U., Balmaseda, M. A., Balsamo, G., Bauer, P., Bechtold, P., Beljaars, A. C. M., van de Berg, L., Bidlot, J., Bormann, N., Delsol, C., Dragani, R., Fuentes, M., Geer, A. J., Healy S. B., Hersbach, H., Hólm, E. V., Isaksen, L., Kallberg, P., Kölher, M., Matricardi, M., McNally, A. P., Morcrette, J. J., Park, B. K., Peubey, C., de Rosnay, P., Tavolato, C., Thépaut, J. N. and Vitart, F.: The ERA-Interim reanalysis: Configuration and performance of the data assimilation system. Q. J. Roy. Meteor. Soc. 137(656): 553-597, 2011.

DeJarnett, N., and Pittman, M.: Protecting the Health and Wellbeing of Communities in a Changing Climate. Proceedings of a Workshop – in Brief. The National Academies Press. 10.17226/24797, 8p, 2017.

De Ridder, K., Lauwaet, D., and Maiheu, B.: UrbClim–A fast urban boundary layer climate model. Urban Clim. 12: 21-48, 2015.

Dickson, E., Baker, J. L., and Hoornweg, D.: Urban risk assessments: understanding disaster and climate risk in cities. The World Bank Publications, 2012.

https://doi.org/10.5194/nhess-2020-240
Preprint. Discussion started: 1 September 2020

Diffenbaugh, N. S., Pal, J. S., Giorgi, F., and Gao, X.: Heat stress intensification in the Mediterranean climate change hotspot. Geophysical Research Letters, 34(11), 2007.

Drobinski, P., Ducrocq, V., Alpert, P., Anagnostou, E., Béranger, K., Borga, M., Braud, I., Chanzy, A., Davolio, S., Delrieu, G., Estournel, C., Filali Boubrahmi, N., Font, J., Grubisic, V., Gualdi, S., Homar, V., Ivancan-Picek, B., Kottmeier, C., Kotroni, V., Lagouvardos, K., Lionello, P., Llasat, M. C., Ludwig, W., Lutoff, C., Mariotti, A., Richard, E., Romero, R., Rotunno, R., Roussot, O., Ruin, I., Somot, S., Taupier-Letage, I., Tintore, J., Uijlenhoet, R. and Wernli, H.: HyMeX, a 10-year multidisciplinary program on the Mediterranean water cycle, B. Am. Meteorol. Soc. 95(7): 1063-1082, 2014.

Eum, J. H., Kim, K., Jung, E. H., and Rho, P.: Evaluation and Utilization of Thermal Environment Associated with Policy: A Case Study of Daegu Metropolitan City in South Korea. Sustainability. 10(4): 1179, 2018.

García Díez, M., Lauwaet, D., Hooyberghs, H., Ballester, J., De Ridder, K., and Rodó, X.: Advantages of using a fast urban boundary layer model as compared to a full mesoscale model to simulate the urban heat island of Barcelona. Geosci. Model Dev. 9(12): 4439-4450, 2016.

Geletič, J., Lehnert, M., Dobrovolný, P.: Land Surface Temperature Differences within Local Climate Zones, Based on Two Central European Cities. Remote Sens. 8(10): 788, 2016.

Geletič, J., Lehnert, M.: GIS-based delineation of local climate zones: The case of medium-sized Central European cities. Morav. Geogr. Rep. 24(3): 2-12, 2016.

Geletič, J., Lehnert, M., Savic, S., and Miloševic, D.: Modelled spatiotemporal variability of outdoor thermal comfort in local climate zones of the city of Brno, Czech Republic. Science of the Total Environment, 624, 385–395, 2018.

Giannaros, T. M., Melas, D., Daglis, I. A., and Keramitsoglou, I.: Development of an operational modeling system for urban heat islands: an application to Athens, Greece. Nat. Hazards Earth Syst. Sci., 14(2), 347, 2014.

Gilabert, J., Tardà, A., Llasat, M. C., and Corbera, J.: Assessment of Local Climate Zones over Metropolitan Area of Barcelona and added value of Urban Atlas, Corine Land Cover and Copernicus Layers under INSPIRE Specifications. INSPIRE Conference, Barcelona, 2016.

Gilabert, J., and Llasat, M. C.: Circulation Weather Types associated with extreme flood events in Northwestern Mediterranean. Int. J. Climatol. 38(4): 1864-1876, 2017.

Hallegatte, S., Green, C., Nicholls, R. J. and Corfee-Morlot, J.: Future flood losses in major coastal cities. Nat. Clim. Change 3, 802–806, 2013.

Hammerberg, K., Brousse, O., Martilli, A., and Mahdavi A.: Implications of employing detailed urban canopy parameters for mesoscale climate modelling: a comparison between WUDAPT and GIS databases over Vienna, Austria. Int. J. of Climatol. 38: 1241-1257, 2018.

Hanson, S., Nicholls, R., Ranger, N., Hallegatte, S., Cofree-Morlot, J., Herweijer, C., Chateau, J.: A global ranking of port cities with high exposure to climate extremes. Climatic Change, 104(1), 89-111, 2011.

Ingole, V., Marí-Dell'Olmo, M., Deluca, A., Quijal, M., Borrell, C., Rodríguez-Sanz, M., Achebak, H., Lauwet, D., Gilabert, J., Murage, P., Hajat, S., Basagaña, X., and Ballester, J.: Spatial Variability of Heat-Related Mortality in Barcelona from 1992–2015: A Case Crossover Study Design. Int. J. Environ. Res. Public Health.17(7): 2553, 2020.

Inostroza, L., Palme, M., and de la Barrera, F.: A heat vulnerability index: spatial patterns of exposure, sensitivity and adaptive capacity for Santiago de Chile. PloS one. 11(9): e0162464, 2016.

Kotharkar, R., Bagade, A.: Local Climate Zone classification for Indian cities: A case study of Nagpur. Urban clim. 24: 369-392, 2018.

Krstic, N., Yuchi, W., Ho, H. C., Walker, B. B., Knudby, A. J., and Henderson, S. B.: The Heat Exposure Integrated Deprivation Index (HEIDI): A data-driven approach to quantifying neighborhood risk during extreme hot weather. Environ. Int. 109: 42-52, 2017.

https://doi.org/10.5194/nhess-2020-240
Preprint. Discussion started: 1 September 2020

Kwok, Y. T., Schoetter, R., Lau, K. K. L., Hidalgo, J., Ren, C., Pigeon, G., and Masson, V.: How well does the local climate zone scheme discern the thermal environment of Toulouse (France)? An analysis using numerical simulation data. International Journal of Climatology, 39(14), 5292-5315, 2019.

Lehoczky, A., Sobrino, J. A., Skoković, D., and Aguilar, E.:The Urban Heat Island Effect in the City of Valencia: A Case Study for Hot Summer Days. *Urban Science*, *1*(1), 9, 2017.

Lelovics, E., Unger, J., and Gál, T.: Design of an urban monitoring network based on Local Climate Zone mapping and temperature pattern modelling. Clim. Res. 60: 51-62.
Li D, Bou-Zeid E. (2013) Synergistic interactions between urban heat islands and heat waves: the impact in cities is larger than the sum of its parts. J. Appl. Meteorol. Clim. 52(9): 2051-2064, 2014.

Li, X., Li, W., Middel, A., Harlan, S. L., Brazel, A. J, and Turner, B. L.: Remote sensing of the surface urban heat island and land architecture in Phoenix, Arizona: Combined effects of land composition and configuration and cadastral- demographic- economic factors. Remote Sens. Environ. 174: 233-243, 2016.

Lionello, P., Abrantes, F., Gacic, M., Planton, S., Trigo, R., and Ulbrich, U.: The climate of the Mediterranean region: research progress and climate change impacts. Reg Environ Change 14, 1679–1684., 2014.

Llasat, M. C., Llasat-Botija, M., López, L.: A press database on natural risks and its application in the study of floods in Northeastern Spain. Nat. Hazard. Earth Sys. 9(6): 2049-2061, 2009.

Lo C. P., Quattrochi, D. A., and Luvall, J. C.: Application of high-resolution thermal infrared remote sensing and GIS to assess the urban heat island effect. Int. J. Remote Sens. 18(2): 287-304, 1997.

Martin-Vide, J., and Moreno-Garcia, M. C.: Probability values for the intensity of Barcelona's urban heat island (Spain). Atmos. Res., 104877, 2020.

https://doi.org/10.5194/nhess-2020-240
Preprint. Discussion started: 1 September 2020

Masterton, J. M., and Richardson, F. A.: Humidex: a method of quantifying human discomfort due to excessive heat and humidity. Environment Canada. Atmospheric Environment, 1979.

MedECC.: Risks associated to climate and environmental changes in the Mediterranean region. A preliminary assessment by the MedECC Network. Science-policy interface – 2019. 36 pp, 2019.

Mirzaei, P. A., Haghighat, F.: Approaches to study urban heat island–abilities and limitations. Build. Environ. 45(10): 2192-2201, 2010.

Mitraka, Z., del Frate, F., Chrysoulakis, N., and Gastellu-Etchegorry, J. P.: Exploiting earth observation data products for mapping local climate zones. Joint Urban Remote Sensing Event (JURSE). 1-4, 2015.

Nakamura, I., and Llasat, M. C.: Policy and systems of flood risk management: a comparative study between Japan and Spain. Nat. Hazards. 87(2): 919-943, 2017.

Nations, United.: World population prospects: The 2015 revision. United Nations Econ. Soc. Aff. 33(2): 1-66, 2015.

Nayak, S. G., Shrestha, S., Kinney, P. L., Ross, Z., Sheridan, S. C., Pantea, C. I., Hsu, W. H., Muscatiello, N., and Hwang, S. A.: Development of a heat vulnerability index for New York State. Public health. 161: 127-137, 2018.

Oke, T. R.: The energetic basis of the urban heat island. Q. J. Roy. Meteor. Soc. 108(455): 1-24, 1982.

Pachauri, R. K., Allen, M. R., Barros, V. R., Broome, J., Cramer, W., Christ, R., Church J. A., Clarke, L., Dahe, Q., Dasgupta, P., Dubash, N. K., Edenhofer, O., Elgizouli, I., Field, C. B., Forster, P., Friedlingstein, P., Fuglestvedt, J., Gomez-Echeverri, L., Hallegatte, S., Hegerl, G., Howden, M., Jiang, K., Jimenez Cisneroz, B., Kattsov, K., Lee, H., Mach, K. J., Marotzke, J., Mastrandrea, M. D., Meyer, L., Minx, J., Mulugetta, Y., O'Brien, Oppenheimer, M., Pereira, J. J., Pichs-Madruga, R., Plattner, G. K., Pörtner, H. O., Power, S. B., Preston, B., Ravindranath, N.H., Reisinger, A., Riahi, K., Rusticucci, M., Scholes, R., Seyboth, K., Sokona, Y., Stavins, R., Stocker, T. F., Tschakert, P., van

https://doi.org/10.5194/nhess-2020-240
Preprint. Discussion started: 1 September 2020

Natural Hazards and Earth System Sciences Open Access
Discussions

Vuuren, D., and van Ypserle, J.P.: Climate change 2014: synthesis report. Contribution of working groups I, II and III to the fifth assessment report of the intergovernmental panel on climate change. R. Pachauri, L. Meyer (Eds.), IPCC, Geneva, Switzerland. ISBN: 978-92-9169-143-2, 2014.

Rosenzweig, C., Solecki, W. D., Romero-Lankao, P., Mehrotra, S., Dhakal, S., and Ali Ibrahim, S.: Climate change and cities. Second assessment report of the urban climate change research network. New York: Cambridge University Press. Retrieved from: http://www.cambridge.org/ws/academic/subjects/earth-and-environmental-science/climatology-and-climate-change/climate-change-and-cities-second-assessment-report-urban-climate-change-research-network, 2018.

Sheridan, S. C., and Dixon, P. G.: Spatiotemporal trends in human vulnerability and adaptation to heat across the United States. Anthropocene. 20: 61-73, 2016.

Skarbit, N., Stewart, I. D., Unger, J., and Gál, T.: Employing an urban meteorological network to monitor air temperature conditions in the 'local climate zones' of Szeged, Hungary. Int. J. Climatol. 37: 582-596, 2017.

Skarbit, N., Gal, T., and Unger, J.: Airborne surface temperature differences of the different Local Climate Zones in the urban area of a medium sized city. Joint Urban Remote Sensing Event (JURSE). 1-4, 2015.

Smid, M., Russo, S., Costa, A. C., Granell, C., and Pebesma, E.: Ranking European capitals by exposure to heat waves and cold waves. Urban Climate, 27, 388-402, 2019.

Sobrino, J. A., and Irakulis, I.: A Methodology for Comparing the Surface Urban Heat Island in Selected Urban Agglomerations Around the World from Sentinel-3 SLSTR Data. Remote Sensing, 12(12), 2052, 20202.

Stewart, I. D.: A systematic review and scientific critique of methodology in modern urban heat island literature. Int. J. Climatol. 31(2): 200-217, 2011.

Stewart, I. D., and Oke, T. R.: Local climate zones for urban temperature studies. B. Am. Meteorol. Soc. 93(12): 1879-1900, 2012.

Stewart, I. D., Oke, T. R., and Krayenhoff, E. S.: Evaluation of the ‘local climate zone’ scheme using temperature observations and model simulations. Int. J. Climatol. 34(4): 1062-1080, 2014.

Tromeur, E., Ménard, R., Bailly, J. B., and Soulié, C.: Urban vulnerability and resilience within the context of climate change. Nat. Hazards Earth Syst. Sci., 12(5), 2012.

Unger, J., Skarbit, N. and Gál, T.: Evaluation of outdoor human thermal sensation of local climate zones based on long-term database. International Journal of Biometeorology, 62(2), 183–193, 2018.

UNISDR, UNOFDRR.: Terminology on disaster risk reduction. Geneva, Switzerland, 2009.

Verdonck, M. L., Demuzere, M., Hooyberghs, H., Beck, C., Cyrys, J., Schneider, A., Dewulf, R., and Van Coillie, F.: The potential of local climate zones maps as a heat stress assessment tool, supported by simulated air temperature data. Landscape Urban plan. 178: 183-197, 2018.

Voogt, J. A., and Oke, T. R.: Thermal remote sensing of urban climates Remote Sens. Environ. 86(3): 370-384, 2003.

Wang, R., Ren, C., Xu, Y., Lau, K. K. L., and Shi, Y.: Mapping the local climate zones of urban areas by GIS-based and WUDAPT methods: A case study of Hong Kong. Urban Clim. 24: 567- 576, 2017.

Weber, S., Sadoff, N., Zell, E., and de Sherbinin A.: Policy-relevant indicators for mapping the vulnerability of urban populations to extreme heat events: A case study of Philadelphia. Appl. Geogr. 63: 231-243, 201.5, 2015.

Wolf, T., and McGregor G.: The development of a heat wave vulnerability index for London, United Kingdom. Weather and Climate Extremes. 1: 59-68, 2013

Xu, Z., Sheffield, P. E., Hu, W., Su, H., Yu, W., Qi, X., and Tong S.: Climate change and children’s health- A call for research on what works to protect children. I Int. J. Environ. Res. Public Health. 9(9): 3298-3316, 2012.

https://doi.org/10.5194/nhess-2020-240
Preprint. Discussion started: 1 September 2020

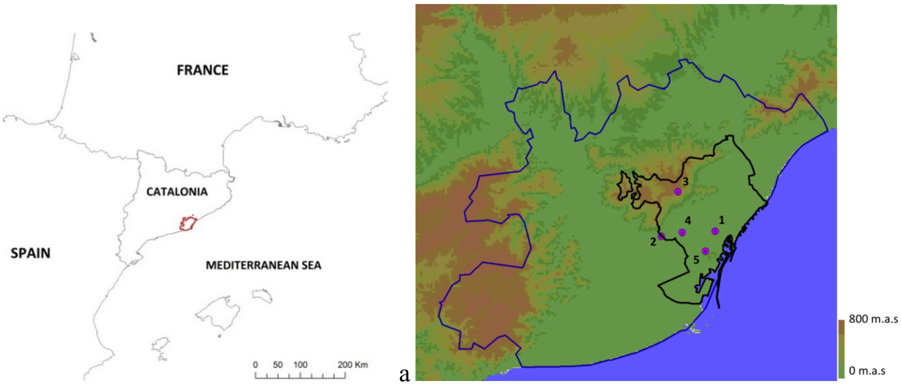

Figure 1. a) Location of the Metropolitan Area of Barcelona (AMB), b) Domain used to run the UrbClim model. The blue line marks the border of the AMB, while the black line shows the municipality of Barcelona. The numbers indicate the weather stations used to assess the LCZ-T relationship.

https://doi.org/10.5194/nhess-2020-240
Preprint. Discussion started: 1 September 2020

Natural Hazards and Earth System Sciences
Open Access
Discussions

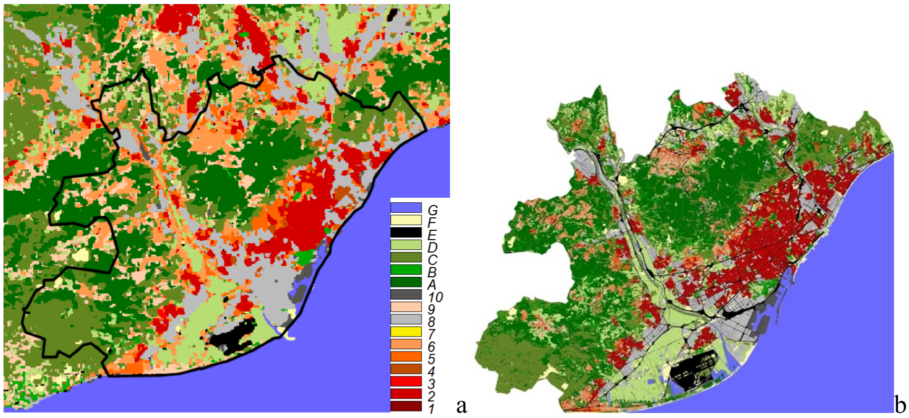

Figure 2. LCZ maps: a) WUDAPT method, b) LCLU method.

https://doi.org/10.5194/nhess-2020-240
Preprint. Discussion started: 1 September 2020

Natural Hazards and Earth System Sciences
Discussions

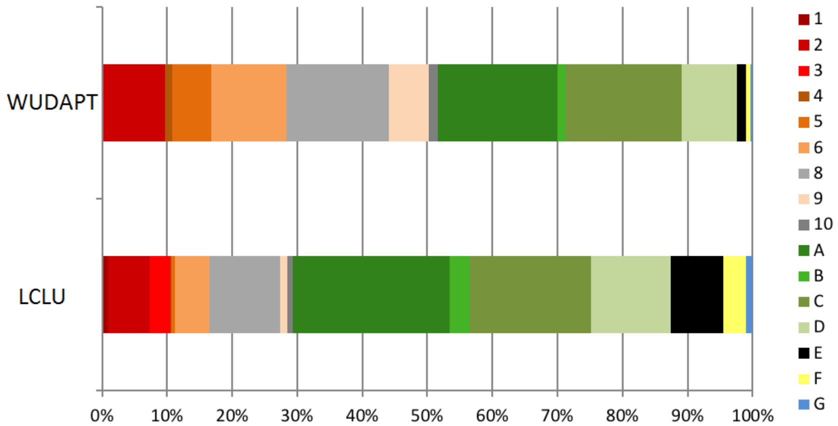

Figure 3. Percentage of the area covered by each LCZ using WUDAPT and LCLU inside AMB.

https://doi.org/10.5194/nhess-2020-240
Preprint. Discussion started: 1 September 2020

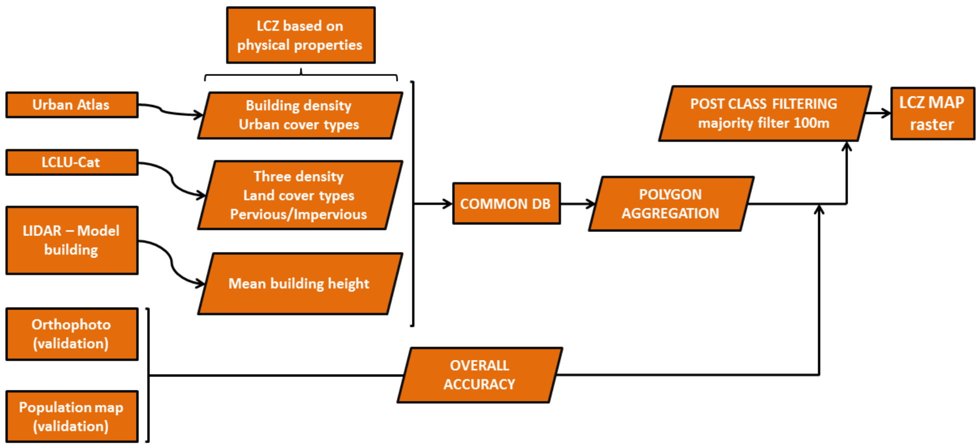

Figure 4. Workflow used to obtain the LCZ LCLU model.

https://doi.org/10.5194/nhess-2020-240
Preprint. Discussion started: 1 September 2020

Natural Hazards and Earth System Sciences
Open Access
Discussions

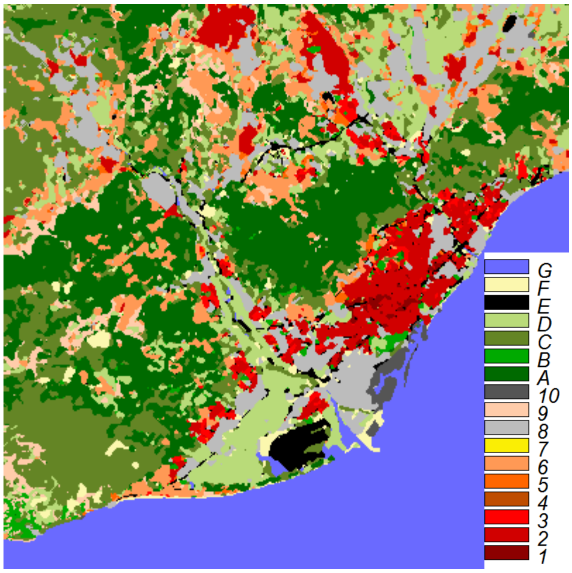

Figure 5. LCZ used in the UrbClim model based on workflow showed in Fig. 4.

https://doi.org/10.5194/nhess-2020-240
Preprint. Discussion started: 1 September 2020

Natural Hazards and Earth System Sciences
Open Access
Discussions

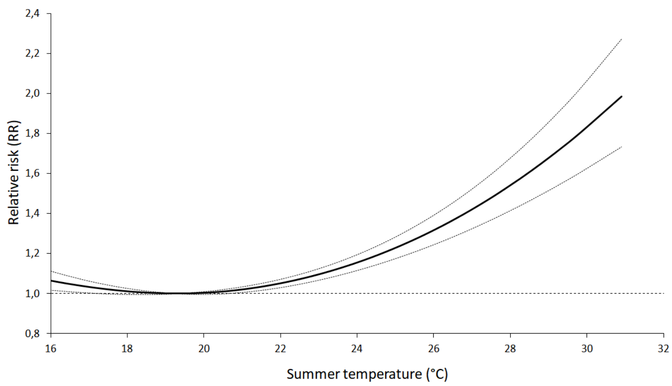

Figure 6. Relative risk (RR) curve based on mortality due to summer daily temperature (JJA) in Barcelona for the 1980 - 2015 period (Achebak et al., 2018).

https://doi.org/10.5194/nhess-2020-240
Preprint. Discussion started: 1 September 2020

Natural Hazards and Earth System Sciences
Open Access
Discussions

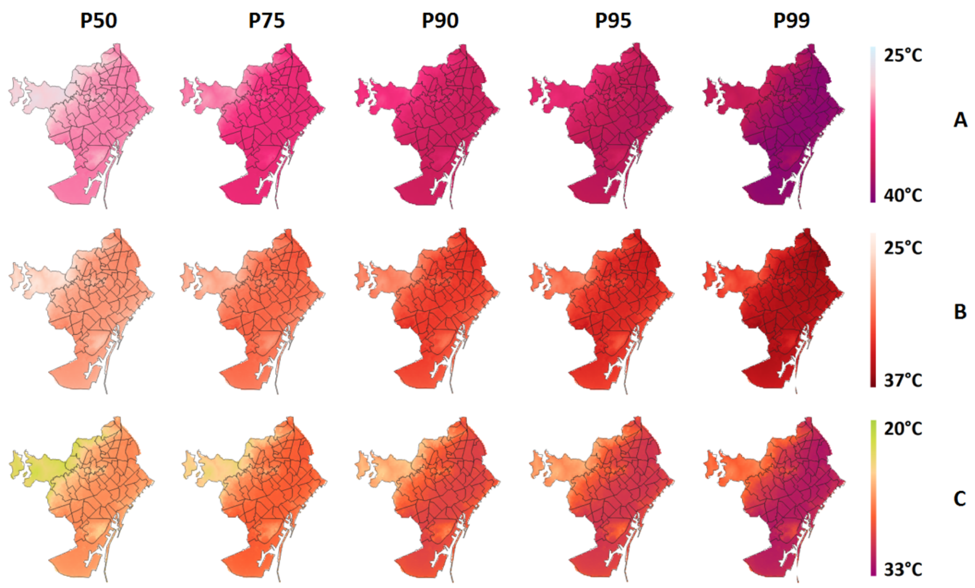

Figure 7. Climatological conditions in summer modelled by UrbClim (1987 - 2016): A) HUMIDEX, B) Daily maximum temperature, C) Daily mean temperature, for the different distributions (P 50, P 75, P 90, P 95 and P 99).

https://doi.org/10.5194/nhess-2020-240
Preprint. Discussion started: 1 September 2020

Natural Hazards and Earth System Sciences
Open Access
Discussions

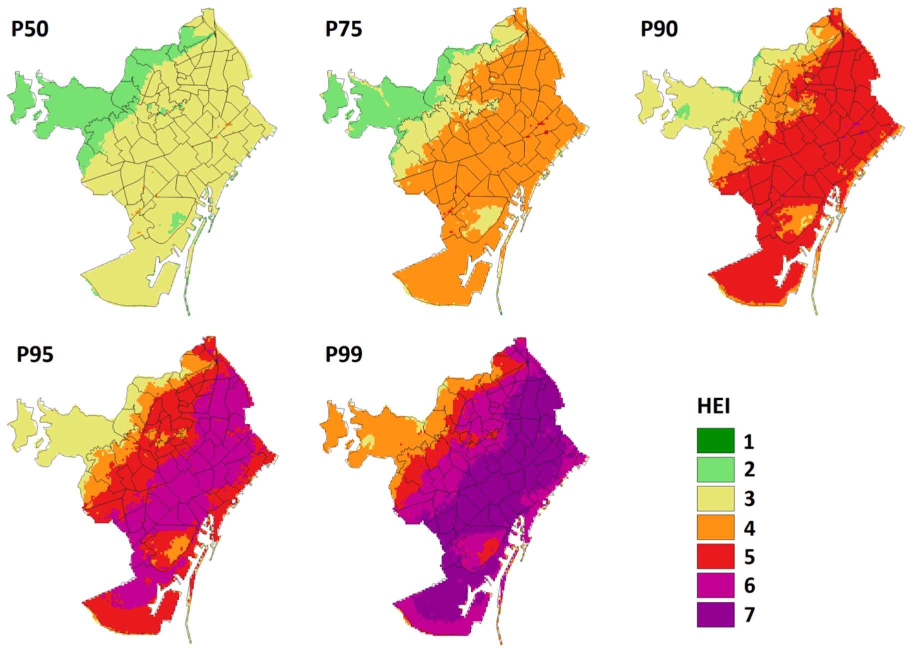

Figure 8. Maps of HEI for the different probability distributions proposed (P 50, P 75, P 90, P 95 and P 99).

https://doi.org/10.5194/nhess-2020-240
Preprint. Discussion started: 1 September 2020

Natural Hazards and Earth System Sciences
Open Access
Discussions

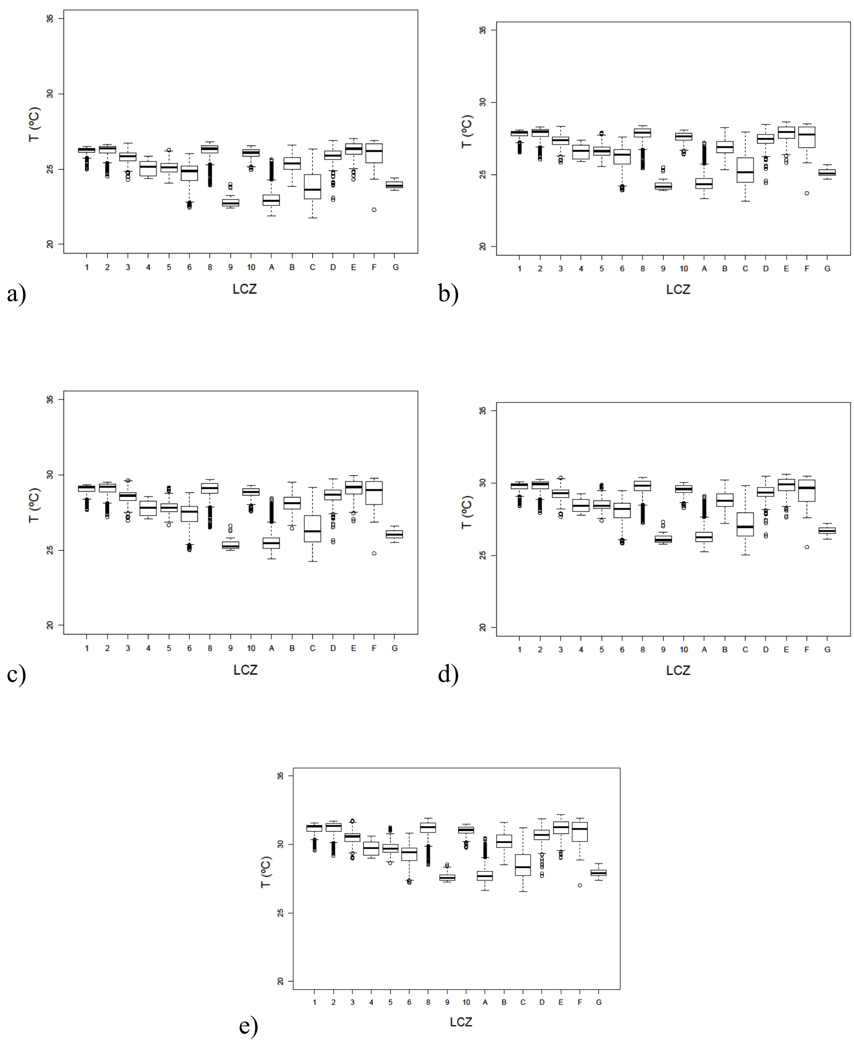

Figure 9. Box plots for the thermal characterisation of the LCZ for different distributions: a) P 50, b) P 75, c) P 90, d) P 95 and e) P 99. (See S1 for LCZ features)

https://doi.org/10.5194/nhess-2020-240
Preprint. Discussion started: 1 September 2020

Natural Hazards and Earth System Sciences
Discussions

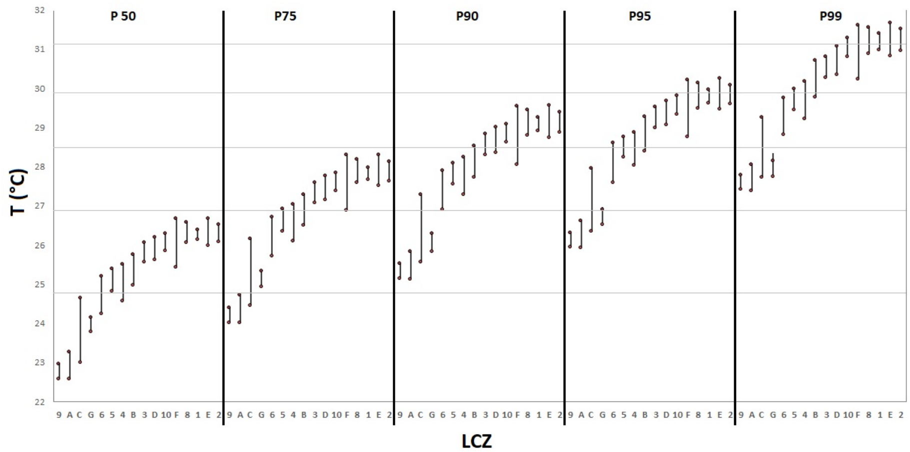

Figure 10. Characterisation of every LCZ with the daily mean temperature (1987 - 2016) for each probability scenario. Each bar shows P 25 and P 75, around the median for each LCZ (ordered from lowest to highest temperature). The grey horizontal lines are the different HEI scenarios (2 to 7, lower to high).

https://doi.org/10.5194/nhess-2020-240
Preprint. Discussion started: 1 September 2020

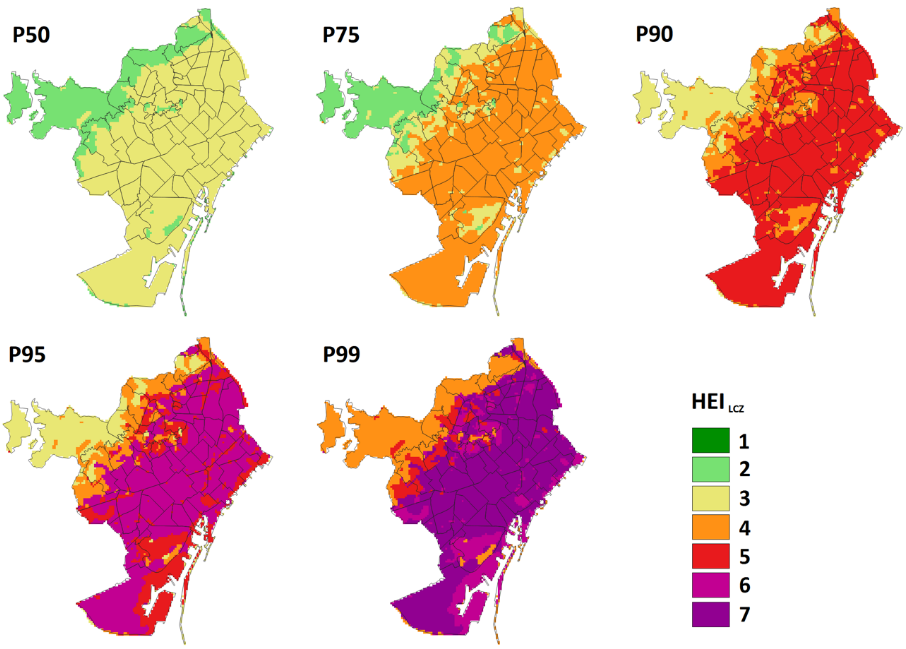

Figure 11. Cartography of the heat exposure (HEI) in basis to thermal characterization of Barcelona by LCZs for different percentiles (LCZ - T) as shown in Table 3.

https://doi.org/10.5194/nhess-2020-240
Preprint. Discussion started: 1 September 2020

Layer	**Information**	**Spatial Resolution**	**Year**	**Format**
Urban Atlas	20 categories of urban fabric	5 m	2010	Vector cartography
LCLU-Cat	241 categories	0.25 m	2010	Vector cartography
Building Heights	Height (m) (LIDAR)	0.5 m	2014	Vector cartography
Orthophoto	Mosaic of aerial photos	0.25 m	2016	Raster cartography
Population	Population by ages	62.5, 125, 250 m	2016	Vector cartography
LANDSAT 8	05/03/2015	30m	2015	Raster satellite

Table 1. Vector and raster cartographic data and satellite images used to map the LCZ - LCLU and LCZ - WUDAPT methods.

https://doi.org/10.5194/nhess-2020-240
Preprint. Discussion started: 1 September 2020

Natural Hazards and Earth System Sciences Discussions

ID	Weather Stations	Series	Years	LCZ	Z (m.a.s)	Variable
1	Raval	1997-2016	19	2	33	T daily
2	Zona Universitària	1997-2016	19	C	79	T daily
3	Fabra	1987-2016	29	A	411	T daily
4	Can Bruixa	1987-2015	28	2	61	T daily
5	Montjuïc	2004-2015	11	B	90	T daily

Table 2. Weather stations in Barcelona used to assess the LCZ - T relationship based on daily mean temperatures.

https://doi.org/10.5194/nhess-2020-240
Preprint. Discussion started: 1 September 2020

Natural Hazards and Earth System Sciences
Discussions

RR	HEI	ºC
1.0	1	18 -20
1.2	2	20 -24.7
1.4	3	24.7 -26.9
1.6	4	26.9 -28.5
1.8	5	28.5 -29.8
2.0	6	29.8 -31.1
>2.0	7	>31.1

Table 3. Temperature thresholds associated to heat exposure caused by high temperatures in basis to figure 5. Heat Exposure Index (HEI) is assigned to each temperature range.

LCZ	P 50	P 75	P 90	P 95	P 99
1	0.301	0.325	0.349	0.363	0.419
2	0.356	0.379	0.396	0.401	0.475
3	0.450	0.468	0.486	0.489	0.552
4	0.528	0.530	0.535	0.522	0.569
5	0.467	0.488	0.504	0.500	0.541
6	0.821	0.841	0.872	0.843	0.804
8	0.465	0.499	0.527	0.531	0.580
9	0.456	0.474	0.461	0.441	0.379
10	0.319	0.338	0.339	0.338	0.322
A	0.686	0.712	0.725	0.705	0.649
B	0.554	0.580	0.603	0.616	0.641
C	1.090	1.128	1.168	1.128	1.088
D	0.550	0.572	0.596	0.586	0.612
E	0.530	0.561	0.599	0.595	0.678
F	0.848	0.918	0.960	0.955	0.978
G	0.224	0.265	0.297	0.294	0.289

Table 4. Standard deviations for the LCZs for the different percentiles of temperature.

https://doi.org/10.5194/nhess-2020-240
Preprint. Discussion started: 1 September 2020

	DIST	OB	UC	LCZ-T	ΔOB–UC	ΔOB–LCZ-T
1-Raval (LCZ 2)	P50	25.6	26.1	26.1	0.5	0.5
	P75	26.8	27.6	27.6	0.8	0.8
	P90	27.8	28.9	28.9	1.1	1.1
	P95	28.5	29.6	29.6	1.1	1.1
	P99	30.2	31.1	30.9	0.9	0.7
2-ZU (LCZ C)	P50	24.5	24.7	24.6	0.2	0.1
	P75	25.8	26.2	26.2	0.4	0.4
	P90	26.6	27.3	27.3	0.7	0.7
	P95	27.2	28.1	27.9	0.9	0.7
	P99	28.5	29.5	29.2	1	0.7
3-Fabra (LCZ A)	P50	23.1	23.1	22.9	0	-0.2
	P75	24.6	24.7	24.3	0.1	-0.3
	P90	25.9	25.8	25.5	-0.1	-0.4
	P95	26.5	26.6	26.2	0.1	-0.3
	P99	27.3	27.5	27.7	0.2	0.4
4-C. Brúixa (LCZ B)	P50	25.2	26.1	25.4	0.9	0.2
	P75	26.8	27.6	26.9	0.8	0.1
	P90	27.9	28.9	28.1	1	0.2
	P95	28.6	29.6	28.8	1	0.2
	P99	30	30.9	30.2	0.9	0.2
5-Montjuïc (LCZ B)	P50	24.8	25.2	25.0	0.4	0.2
	P75	26.3	26.8	26.5	0.5	0.2
	P90	27.3	28	27.7	0.7	0.4
	P95	27.8	28.6	28.4	0.8	0.6
	P99	29.1	30.1	29.8	1	0.7

Table 5. Temperature for each distribution/scenario (DIST) and weather station observed (OB), modelled by UrbClim (UC) and estimated from the distribution of temperature (the mean value is taken) for each LCZ (LCZ-T). The difference (Δ) between them is also showed. All the values are expressed in º C.

https://doi.org/10.5194/nhess-2020-240
Preprint. Discussion started: 1 September 2020

MODEL	P50	P75	P90	P95	P99
Underestimate	284	671	1711	2789	2289
Good	9687	8762	8175	6316	6823
Overestimate	247	785	332	1103	1106
% correct	95	86	80	62	67
RMSE	0.23	0.38	0.45	0.62	0.58

Table 6. Number of pixels where the HEI obtained through the LCZ-T model (Figure 11) underestimate, overestimate or coincide with the HEI provided by the Urban Climate Model (Figure 6) for the different scenarios. Percentage of coincidences and RMSE are also showed.